

Detecting a light Higgs boson at the Fermilab Tevatron through enhanced decays to photon pairs

Stephen Mrenna and James Wells

Davis Institute for High Energy Physics, University of California, Davis, California 95616

(Received 26 January 2000; published 1 December 2000)

We analyze the prospects of the Fermilab Tevatron for finding a Higgs boson in the two photon decay mode. We conclude that the standard model (SM) Higgs boson will likely not be discovered in this mode. However, we motivate several theories beyond the SM, including the MSSM, which predict a Higgs boson with enhanced branching fractions into photons, and calculate the luminosity needed to discover a general Higgs boson at the Tevatron by a two-photon invariant mass peak at large transverse momentum. We find that a high luminosity Tevatron will play a significant role in proving or constraining these theories.

DOI: 10.1103/PhysRevD.63.015006

PACS number(s): 14.80.Cp

INTRODUCTION

In this paper, we investigate the possibility that the Higgs boson(s) h associated with electroweak symmetry breaking may be found in the $h \rightarrow \gamma\gamma$ decay channel at the Fermilab Tevatron. Our intention is to augment the many important studies preceding and associated with the run II at the Tevatron [1]. In these studies, standard model Higgs boson detectability has been studied vigorously in its most promising production and decay channels. The classic channel of $p\bar{p} \rightarrow Wh \rightarrow l\nu b\bar{b}$ remains the most important channel in the search for the SM Higgs boson; yet other modes can contribute to the total signal significance and perhaps yield evidence for the Higgs boson if sufficient luminosity is attained.

We wish to study in detail the Higgs boson decays to two photons for many reasons. First, in our estimation this decay mode has not received adequate attention in previous studies. The capabilities of Higgs boson discovery in this mode should be carefully documented in order to better understand the Tevatron's full potential for Higgs boson detection. Second, there are many interesting and motivated theories that predict an enhanced decay rate into the $\gamma\gamma$ channel and simultaneous suppression of the $h \rightarrow b\bar{b}$ channel. Therefore, in these cases, non-standard search strategies must be employed to either find this Higgs boson or rule out its existence in the kinematically accessible mass range. And finally, we feel that studies such as these contribute to a more knowledgeable discussion regarding the worth of a higher luminosity Tevatron (e.g., run III).

Since there is no renormalizable and gauge invariant operator in the standard model that leads to $h \rightarrow \gamma\gamma$ decays, it must be induced by electroweak symmetry breaking effects. The decay proceeds mainly through loop diagrams containing W^\pm bosons and the t quark. The W^\pm boson loop is dominant. The branching fraction for this decay in the light Higgs boson mass range $100 \lesssim m_h \lesssim 150$ GeV is never much larger than 10^{-3} since the $\gamma\gamma$ partial width must compete with the larger partial widths associated with $b\bar{b}$, $\tau^+\tau^-$, $c\bar{c}$, gg , and WW^* decays. The branching fractions for the standard model Higgs boson have been reliably calculated in Ref. [2]. The maximum of the standard model branching fraction is 0.22% and is reached at $m_h = 125$ GeV. For m_h

> 125 GeV, the branching fraction falls somewhat rapidly due to the increased importance of WW^* decays.

BEYOND THE STANDARD MODEL

It is widely recognized that the standard model is an unsatisfactory explanation of electroweak symmetry breaking. In this section, we review several well-motivated alternatives to the standard model Higgs sector. The first of these is low-scale supersymmetry, where the symmetry breaking tasks are shared by two fields: H_u and H_d . H_u receives a vacuum expectation value and gives mass to the up-type quarks, while H_d receives a vacuum expectation value and gives mass to the down-type quarks. Both $\langle H_u \rangle$ and $\langle H_d \rangle$ vacuum expectation values contribute to the W^\pm and Z^0 masses. In general, the sharing of the electroweak symmetry breaking task between two or more fields will disrupt expectations of Higgs boson phenomenology based solely on the analysis of the standard model Higgs boson. It is important to identify regions of parameter space where our naive expectations fail, and where a more expansive search strategy must be engaged to find evidence of a Higgs boson.

The mass matrix for the CP -even neutral Higgs bosons of supersymmetry in the $\{H_d^0, H_u^0\}$ interaction basis is

$$\mathcal{M}^2 = \begin{pmatrix} m_A^2 \sin^2 \beta + m_Z^2 \cos^2 \beta & -\sin \beta \cos \beta (m_A^2 + m_Z^2) \\ -\sin \beta \cos \beta (m_A^2 + m_Z^2) & m_A^2 \cos^2 \beta + m_Z^2 \sin^2 \beta \end{pmatrix} + \begin{pmatrix} \Delta_{dd} & \Delta_{ud} \\ \Delta_{ud} & \Delta_{uu} \end{pmatrix}, \quad (1)$$

where m_A^2 represents the pseudo-scalar mass, whose value is set by supersymmetry breaking, and Δ_{ij} are quantum corrections whose form can be extracted from Ref. [3].

In the limit $m_A \gg m_Z$ the mass eigenstates of the above mass matrix are

$$h_{\text{light}}^0 = \cos \beta H_d^0 + \sin \beta H_u^0 \quad (2)$$

$$h_{\text{heavy}}^0 = -\sin \beta H_d^0 + \cos \beta H_u^0. \quad (3)$$

One can immediately see that $\langle h_{\text{light}}^0 \rangle = v$ and $\langle h_{\text{heavy}}^0 \rangle = 0$, and it is also true that all interactions of h_{light}^0 are equivalent

to the SM Higgs boson. It is instructive to rotate the Higgs boson mass matrix to the $\{h_{\text{light}}^0, h_{\text{heavy}}^0\}$ basis,

$$\mathcal{M}'^2 = \begin{pmatrix} m_Z^2 \cos^2 2\beta & -m_Z^2 \sin 2\beta \cos 2\beta \\ -m_Z^2 \sin 2\beta \cos 2\beta & m_A^2 + m_Z^2 \sin^2 2\beta \end{pmatrix} + \begin{pmatrix} \Delta'_{11} & \Delta'_{12} \\ \Delta'_{12} & \Delta'_{11} \end{pmatrix}, \quad (4)$$

where the Δ'_{ij} can be expressed in terms of the more commonly given corrections Δ_{ij} :

$$\begin{aligned} \Delta'_{11} &= \Delta_{dd} \cos^2 \beta + 2\Delta_{ud} \cos \beta \sin \beta + \Delta_{uu} \sin^2 \beta \\ \Delta'_{12} &= -\Delta_{dd} \cos \beta \sin \beta + \Delta_{ud} \cos 2\beta + \Delta_{uu} \cos \beta \sin \beta \\ \Delta'_{22} &= \Delta_{dd} \sin^2 \beta - 2\Delta_{ud} \cos \beta \sin \beta + \Delta_{uu} \cos^2 \beta. \end{aligned}$$

“Higgs decoupling” in supersymmetry means that one Higgs boson stays light and couples just like the SM Higgs boson as supersymmetry breaking mass scales get very high. This property of the supersymmetric Higgs sector can be immediately understood as a complete $SU(2)$ Higgs doublet becoming very heavy ($h_{\text{heavy}}^0, A^0, H^\pm$), while another doublet stays light ($h_{\text{light}}^0, Z_L^0, W_L^\pm$). In the expressions above, this is equivalent to noting that m_A^2 occurs only in the \mathcal{M}'_{22} element of the $h_{\text{light}}^0 - h_{\text{heavy}}^0$ mass matrix.

In supersymmetry model building, the supersymmetry breaking scale is a free parameter and is cycled over a very large range. This gives the false impression that over the vast majority of the parameter space, m_A is sufficiently larger than m_Z to be in the “decoupling region” described in the previous two paragraphs, and the lightest Higgs boson is well approximated by h_{light}^0 . However, a natural electroweak potential — meaning a potential that has no large cancellations to produce the Z boson mass — prefers supersymmetry breaking near the weak scale. If we take naturalness and fine tuning arguments seriously, we expect $m_A \sim m_Z$, which leads to potentially significant deviations of the light Higgs boson couplings to the SM particles.

An interesting departure from SM Higgs phenomenology occurs when the light Higgs boson mass eigenstate of supersymmetry is the weak eigenstate h_u^0 [4–7]. This scenario, or close approximations to it, can naturally occur in theories with large $\tan \beta = \langle H_u \rangle / \langle H_d \rangle$, which are motivated by supersymmetric $SO(10)$ unification [8], and by minimal gauge-mediated supersymmetry theories that solve the soft CP -violating phase problem [9]. The h_u^0 eigenstate has no tree-level coupling to $b\bar{b}$ or $\tau^+\tau^-$, and the total width for this light Higgs boson is greatly reduced. Loop corrections can modify these arguments. For example, supersymmetry breaking can induce couplings such as $\lambda'_b H_u^* b\bar{b}$ (and $\lambda'_\tau H_u^* b\bar{b}$) in addition to the usual $\lambda_b H_d b\bar{b}$. The most important of these corrections often comes from gluino-squark loops (which do not contribute to λ'_τ).

If a significant λ'_b coupling is induced, the condition for shutting off the $b\bar{b}$ coupling is to shift the Higgs rotation

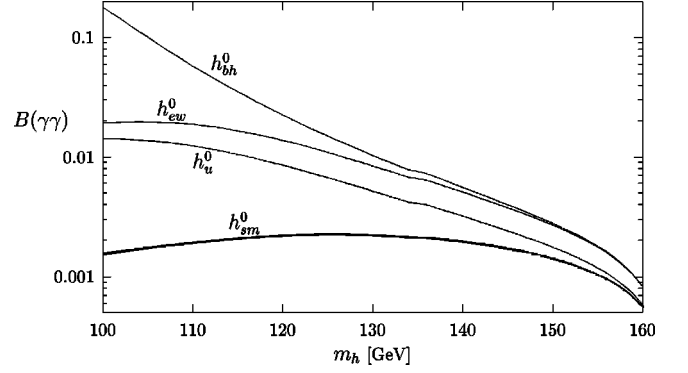


FIG. 1. Branching fraction into two photons for four different types of Higgs bosons: (1) h_{sm}^0 is the standard model Higgs boson, (2) h_u^0 is the Higgs boson with Yukawa couplings only with up-type fermions, which can be a mass eigenstate in large $\tan \beta$ supersymmetric theories, (3) h_{ew}^0 is the Higgs boson that may help complete top quark condensation models as described in the text, and (4) h_{bh}^0 is a Higgs boson with tree level couplings only to W and Z bosons.

angle to $\tan \alpha = \epsilon / \tan \beta$ (or $\tan \alpha = -\epsilon / \tan \beta$ for the case when the heavier CP even Higgs boson is standard model like) where $\epsilon \equiv \Delta m_b / (m_b - \Delta m_b)$ and $\Delta m_b \equiv \lambda'_b \langle H_u \rangle$. The $\tau\tau$ branching is not zero now, but is modified by a factor of ϵ^2 compared to the standard model (in the limit that λ'_τ is small). In contrast to the suppressed down-type fermion couplings, the partial width to two photons is equal to that of the standard model since no down-type quarks or leptons contribute significantly to the loop diagrams in either case. For these reasons, the branching ratio for the two photon final state can be greatly enhanced. Furthermore, the production rates through $gg \rightarrow h_u^0$ and $q\bar{q}' \rightarrow Wh_u^0$ are the same as in the standard model, since neither of these rely on the down-type fermion couplings.

Other interesting theories imply enhanced branching fractions to two photons. The bosonic Higgs field h_{bh}^0 that gives all [10], or rather nearly all, the mass to the vector bosons and has no couplings to fermions is a good example of a Higgs boson with enhanced branching fractions to two photons. However, the production cross section of $gg \rightarrow h_{\text{bh}}^0$ is negligible in this model since the top quark does not couple to this Higgs boson. One must rely completely on electroweak boson couplings for production of the h_{bh}^0 , such as in $q\bar{q}' \rightarrow Wh_{\text{bh}}^0$ or $WW \rightarrow h_{\text{bh}}^0$.

Another example that has suppressed couplings to the fermions is an electroweak Higgs boson h_{ew}^0 added to top-quark condensate models [11]. In this approach, the top and bottom quarks are assumed to get their masses through a strongly coupled group that condenses top quark pairs [12], and all the remaining fermions and vector bosons get mass mainly through $\langle h_{\text{ew}}^0 \rangle$. A good approximation in studying the phenomenology of a light h_{ew}^0 is to assume that it couples like the standard model Higgs boson to all particles except the top quark and bottom quark, to which it has zero couplings.

In Fig. 1 we plot the branching fraction into two photons for the four Higgs bosons that we mentioned above: h_{sm}^0 , h_{bh}^0 , h_u^0 , and h_{ew}^0 . In each non-SM case considered, the

branching fraction is larger than that of h_{sm}^0 . Some models that we have not discussed here may have even higher branching fraction or perhaps lower. It should be kept in mind that *any* model of physics beyond the simple standard model will likely have different branching fractions into two photons. Since the two photon partial width is a one-loop process, it will also be sensitive to new particles in loop diagrams. Hence, even greater variability is possible than what we have shown here. For example, supersymmetric partners in the loops may increase or decrease the overall partial width of $h \rightarrow \gamma\gamma$ [13–15]. In general, we should be prepared to discover and study a Higgs boson with any branching fraction to two photons, since that is perhaps the most likely branching fraction to be altered significantly by new physics.

There are several sizable sources of Higgs boson production within the standard model. At the Tevatron, they are $gg \rightarrow h$, which is the largest, followed by $q\bar{q}' \rightarrow Wh$ and $q\bar{q} \rightarrow Zh$. For a heavy enough Higgs boson, the vector boson fusion processes $WW, ZZ \rightarrow h$ are also competitive. Although the decay branching fraction of $h \rightarrow \gamma\gamma$ is of order $g^2/16\pi^2$, there is hope that the narrow $M_{\gamma\gamma}$ peak of the signal can be utilized to cut extraneous two photon backgrounds to sufficiently low levels that a signal can be detected. In the following two sections, we discuss search strategies based on inclusive and exclusive final states. A description of our calculational methods is provided in the Appendix.

INCLUSIVE $\gamma\gamma+X$ PRODUCTION

First, we consider the total inclusive production of Higgs bosons, followed by their prompt decay to $\gamma\gamma$, where all Higgs boson production mechanisms can contribute. To study inclusive production, we apply cuts only on the properties of the individual photons or the photon pair, without studying the rest of the event in great detail. Before applying any cuts, the photon energy E^γ is smeared by a resolution function typical of run I conditions [16]:

$$\frac{\Delta E^\gamma}{E^\gamma} = \frac{0.15}{\sqrt{E^\gamma} \text{ (GeV)}} \oplus 0.03. \quad (5)$$

To optimize the acceptance of signal events, while reducing the ‘‘irreducible’’ backgrounds and those from jets fragmenting to photons, we apply the cuts

$$p_T^\gamma > 20 \text{ GeV}, |\eta^\gamma| < 2 \quad (\text{triggering and acceptance}),$$

$$\Delta R^{\gamma\gamma} \equiv \sqrt{(\eta_1^\gamma - \eta_2^\gamma)^2 + (\phi_1^\gamma - \phi_2^\gamma)^2} > 0.7 \quad (\text{separation}),$$

$$\sum_{(i), R < 0.4} E_T^{(i)} - p_T^\gamma < 2 \text{ GeV} \quad (\text{isolation}). \quad (6)$$

The sum (i) is over all stable particles within a cone of size $R=0.4$ centered on the γ candidate. The high p_T , central photons constitute a suitable trigger. We failed to find a more efficient p_T^γ cut than the one listed. With these cuts, the dominant source of background comes from the $q\bar{q} \rightarrow \gamma\gamma$

process. For each event, we treat the diphoton pair as a Higgs boson candidate with mass $M_{\gamma\gamma}$.

A further cut on the angular distribution of the photons in the rest frame of the Higgs boson candidate increases S/B :

$$|\cos \theta^*| < 0.7. \quad (7)$$

The angle θ^* is defined to be the angle that the photon makes with the *boost* direction in the $\gamma\gamma$ rest frame. The signal is rather flat in $\cos \theta^*$ whereas the raw background peaks at $|\cos \theta^*|=1$. This cut is somewhat redundant to the other acceptance cuts, but will suppress fake backgrounds.

With the above cuts it would require well over 100 fb^{-1} of integrated luminosity to even rule out a SM Higgs boson (95% C.L.) at any mass (the details will be given later). Therefore, new physics that provides a significant enhancement of the $\gamma\gamma+X$ total rate is required for this kind of signal process to be a relevant search. Large enhancements can occur either in the production cross sections or in the decay branching fraction to photons. In the standard model, the $gg \rightarrow h$ process constitutes roughly two-thirds of the total production rate up to about $m_h = 160 \text{ GeV}$, while the rest of the rate is mainly $q\bar{q} \rightarrow W/Z+h$ production. One does not expect the production cross sections $q\bar{q} \rightarrow W/Z+h$ to ever greatly exceed the SM production cross section given the nature of Higgs boson couplings to electroweak vector bosons. One does expect, however, that the $gg \rightarrow h$ rate could be greatly enhanced by an increased coupling of the top quarks to Higgs bosons [17] or by many virtual states contributing to the one-loop, effective ggh coupling, or from higher dimensional operators induced in theories with large extra dimensions [18]. In fact, these effects that increase the rate of $gg \rightarrow h$ production will usually also alter the $h \rightarrow \gamma\gamma$ branching fraction. Therefore, we focus on the possibility of large enhancements of the ratio

$$R_{gg} = \frac{\sigma(gg \rightarrow h)B(h \rightarrow \gamma\gamma)}{\sigma(gg \rightarrow h)_{\text{sm}}B(h \rightarrow \gamma\gamma)_{\text{sm}}}. \quad (8)$$

In the following we will investigate the inclusive $\gamma\gamma+X$ rate from $gg \rightarrow h$ signal production alone. Although this underestimates the total cross section by not taking into account the $W/Z+h$ and $WW, ZZ \rightarrow h$ contributions, it lends itself to easy generalizations of $R_{gg} \gg 1$ where there is hope to find a signal at reasonable luminosity and where the other contributions are very small in comparison. Later on, we will see that the $q\bar{q} \rightarrow W/Z+h$ signature alone lends itself to a useful, complementary analysis based on exclusive final states. In Table I we list the total SM signal cross section ($gg \rightarrow h$ only) and the differential background rate after all cuts have been applied.

The Higgs boson width in the standard model is less than 20 MeV for $m_h < 150 \text{ GeV}$. Therefore, the invariant mass measurement of the two photons will have a spread entirely due to the photon energy resolution of the detector, which we call $\Delta M_{\gamma\gamma}$. In Table II we show $\Delta M_{\gamma\gamma}$ for various Higgs boson masses, based on folding the photon energy resolution function, Eq. (5), with the photon kinematics.

TABLE I. The total $\gamma\gamma+X$ production rate (in fb) for a standard model Higgs boson and the differential rate (in fb per GeV) for the standard model backgrounds after applying cuts, Eqs. (6),(7).

| m_h [GeV] | $\sigma_{\text{sig}}(\gamma\gamma+X)$ [fb] | $d\sigma_{\text{bkgd}}/dM_{\gamma\gamma}$ [fb/GeV] |
|-------------|--|--|
| 100 | 1.49 | 39.3 |
| 110 | 1.43 | 27.6 |
| 120 | 1.29 | 20.2 |
| 130 | 1.02 | 15.1 |
| 140 | 0.73 | 12.3 |
| 150 | 0.42 | 9.8 |
| 160 | 0.13 | 7.4 |
| 170 | 0.029 | 5.7 |

Based on Tables I and II, we are now able to determine the significance of the signal with respect to background after all cuts. We use the formula

$$N_S = \frac{S}{\sqrt{B}} = \frac{0.96\sigma_{\text{sig}}\sqrt{\mathcal{L}}}{\sqrt{\hat{\sigma}_{\text{bkgd}}}}, \quad (9)$$

where

$$\hat{\sigma}_{\text{bkgd}} = 4\Delta M_{\gamma\gamma} \frac{d\sigma_{\text{bkgd}}}{dM_{\gamma\gamma}}, \quad (10)$$

and \mathcal{L} is the integrated luminosity. This formula counts the significance of signal to background within a mass window $M_{\gamma\gamma} \pm 2\Delta M_{\gamma\gamma}$. This is a conservative and simple choice. When both the signal and background can be described adequately using Gaussian statistics, the signal itself has a Gaussian shape, and the background is constant, the mass window yielding the optimal significance N_S is $M_{\gamma\gamma} \pm \sqrt{2}\Delta M_{\gamma\gamma}$. In our case, the background is not a constant, but the differential distribution is well approximated by a straight line with a negative slope. Therefore, an asymmetric mass window (with respect to the peak) would most likely yield the best significance. We also require everywhere in our analysis that no limit or discovery capability be possible unless at least 5 events are present in this 2σ spread mass bin. On the graphs we show below, this is a limitation mainly for the 2 fb^{-1} integrated luminosity curve. From Eqs. (9) and (10), it is worth noting that an increase in integrated luminosity is equivalent to an improved energy resolution.

In Fig. 2 we plot the 95% C.L. ($N_S=1.96$) exclusion curves for a given luminosity in the $R_{gg}-m_h$ plane. The SM Higgs boson corresponds to $R_{gg}=1$ across the plot. We have put on a line on the graph corresponding to h_u^0 to give a non-SM reference example of R_{gg} . Other theories such as

TABLE II. The invariant mass resolution for a narrow signal from our simulations. The resolution is the 1σ value of a Gaussian fit to the simulated signal after applying cuts, Eqs. (6),(7).

| m_h [GeV] | 100 | 110 | 120 | 130 | 140 | 150 | 160 | 170 |
|---------------------------------|------|------|------|------|------|------|------|------|
| $\Delta M_{\gamma\gamma}$ [GeV] | 1.52 | 1.64 | 1.76 | 1.88 | 1.99 | 2.08 | 2.23 | 2.47 |

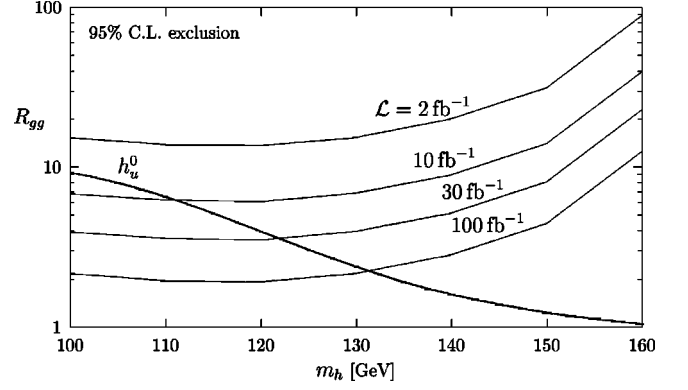


FIG. 2. 95% C.L. luminosity contours of Higgs boson detection in the $R_{gg}-m_h$ plane. For a given luminosity curve, the region below the curve cannot be ruled out with Tevatron data.

those discussed above can have R_{gg} much greater than that of h_{sm}^0 or h_u^0 . The plot is intended to be useful for comparing any theory to Tevatron capabilities. For a given integrated luminosity, the region above the corresponding curve can be ruled out to a 95% confidence level. Therefore, with 30 fb^{-1} one could exclude a h_u^0 up to 120 GeV. The solid lines never cross $R_{gg}=1$ which indicates that the SM Higgs boson could not be excluded in the $\gamma\gamma$ mode by the Tevatron even with over 100 fb^{-1} of data. One interesting limit to consider is a Higgs boson with only one-loop decays to gg and $\gamma\gamma$ final states. In this case, the production cross section \times branching ratio is proportional to $\Gamma(h \rightarrow gg)BR(h \rightarrow \gamma\gamma) \approx \Gamma(h \rightarrow \gamma\gamma)$, and $R_{gg} = \Gamma(h \rightarrow \gamma\gamma)/\Gamma(h_{\text{SM}} \rightarrow gg)BR(h_{\text{SM}} \rightarrow \gamma\gamma) \approx 10^3 \Gamma(h \rightarrow \gamma\gamma)/\Gamma(h_{\text{SM}} \rightarrow gg)$. Therefore, large values of R_{gg} are not unreasonable.

The discovery of Higgs bosons with enhanced $\gamma\gamma+X$ production rates requires higher significance. For $N_S=5$ we plot in Fig. 3 the necessary enhancement R_{gg} to see a signal at this level at the Tevatron. With less than 30 fb^{-1} , discovery is not likely for a h_u^0 Higgs boson with mass greater than 100 GeV. Therefore, the Tevatron detection sensitivity in this channel is not as good as the Higgs boson search capacity at CERN e^+e^- collider LEP2 [19], which should exceed 105 GeV for both h_{sm}^0 and h_u^0 . Nevertheless, other theories

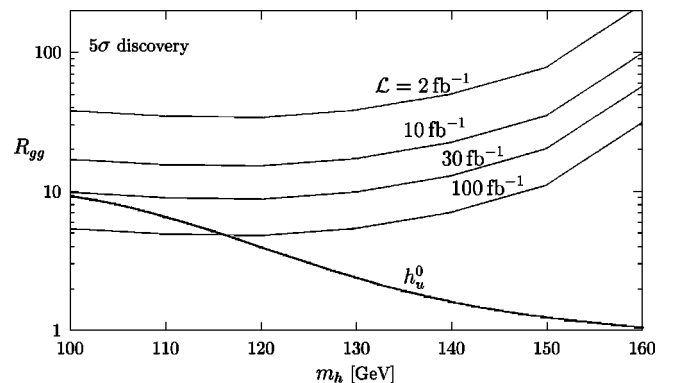


FIG. 3. 5σ discovery contours of Higgs boson detection in the $R_{gg}-m_h$ plane for a given luminosity. For each luminosity curve, the region above the curve can be discovered with Tevatron data.

with larger enhancements of $\sigma(gg \rightarrow h)B(h \rightarrow \gamma\gamma)$ may be discovered in the $\gamma\gamma + X$ mode first.

EXCLUSIVE $W/Z+h \rightarrow W/Z+\gamma\gamma$ SIGNAL OF HIGGS BOSONS

We now attempt to gain more significance of signal to background by employing additional cuts. It is well known that the kinematics of resonance production at hadron colliders can be significantly affected by multiple soft gluon emission. Because of the different color factors associated with the $q\bar{q} \rightarrow \gamma\gamma$ and $gg \rightarrow h$ processes, the $p_T^{\gamma\gamma}$ spectrum of the Higgs boson signal is harder than the background. One strategy of CERN Large Hadron Collider (LHC) searches is to exploit this difference to establish a Higgs signal [20]. However, the process $W/Z+h \rightarrow W/Z+\gamma\gamma$ typically has large $p_T^{\gamma\gamma}$ even before including these QCD effects. At the Tevatron collider, the $W/Z+h$ production process is relatively much more important than at the LHC, and quickly becomes the dominant process at even moderate values of $p_T^{\gamma\gamma}$ with respect to $M_{\gamma\gamma}$. For this reason, and because many of the extensions of the SM considered here have no $gg \rightarrow h$ component or only one of SM strength, we concentrate only on the $W/Z+h$ signal in the following. For reasons discussed later, the $WW/ZZ \rightarrow h$ signal is not as relevant for our analysis.

We have done an analysis of varying the $p_T^{\gamma\gamma}$ cut to maximize the total signal significance. We find that we optimally retain a significant portion of the total Higgs boson signal while reducing the backgrounds with the requirement

$$p_T^{\gamma\gamma} > M_{\gamma\gamma}/2. \quad (11)$$

Also, the two photons from the Higgs boson decay tend to be balanced in p_T , so we demand

$$p_T^{\gamma} > M_{\gamma\gamma}/3 \quad (12)$$

as a further aid to reduce backgrounds and increase S/B .

After demanding such a significant cut on $p_T^{\gamma\gamma}$, the dominant background becomes a $\gamma\gamma+1$ jet. However, the signal will most likely *not* have this topology. Rather, the decay of W and Z bosons can lead to (1) two hard jets with $M_{jj} \approx M_W, M_Z$, (2) one or more high p_T leptons from $W \rightarrow e, \mu$ and $Z \rightarrow ee, \mu\mu$, or (3) missing transverse energy from $Z \rightarrow \nu\nu$, $W \rightarrow \tau \rightarrow$ soft jet, and $W \rightarrow e, \mu \rightarrow$ soft or very forward leptons. Therefore, it is useful to consider $\gamma\gamma$ signals that have one or two leptons, *or* missing energy, *or* two leading jets with $M_{j_1 j_2} \approx m_W, m_Z$. To this end we require at least one of the following ‘‘vector boson acceptance’’ criteria to be satisfied:

- (a) $p_T^{e,\mu} > 10$ GeV and $|\eta^{e,\mu}| < 2.0$.
- (b) $E_T > 20$ GeV.
- (c) 2 or more jets with $50 \text{ GeV} < M_{j_1 j_2} < 100$ GeV.

To perform this analysis, we constructed jets ($E_T^j > 15$ GeV, $|\eta^j| < 2.5$ and $R=0.5$) using the toy calorimeter simulation in PYTHIA with an energy resolution of $80\%/\sqrt{E^j}(\text{GeV})$. E_T was calculated by summing all calorim-

TABLE III. The total signal (in fb) for $\gamma\gamma+V$, where V represents additional states passing the ‘‘vector boson acceptance’’ criteria enumerated in the text. The last column is the calculated background given the same cuts.

| m_h [GeV] | $\sigma_{\text{sig}}(\gamma\gamma+V)$ [fb] | $d\sigma_{\text{bkgd}}/dM_{\gamma\gamma}$ [fb/GeV] |
|-------------|--|--|
| 100 | 0.157 | 0.102 |
| 110 | 0.139 | 0.070 |
| 120 | 0.114 | 0.047 |
| 130 | 0.090 | 0.034 |
| 140 | 0.057 | 0.026 |
| 150 | 0.030 | 0.020 |
| 160 | 0.0092 | 0.014 |
| 170 | 0.0020 | 0.011 |

eter cells out to $\eta=4$. The mass window in (c) was determined from the results of our simulation, and includes the loss of jet energy from radiation outside of the defining cone R and from neutrinos.

The vector boson acceptance cuts eliminate a fair portion of the $\gamma\gamma$ plus jet background, as well as a potential contribution from vector boson fusion. The total rate of the vector fusion process (without cuts) is comparable to $W/Z+h$ only for $M_h > 160$ GeV, where large values of $B(h \rightarrow \gamma\gamma)$ are not well motivated (see, e.g., Fig. 1). Nonetheless, we examined the effects of replacing cuts (a)–(c) by the requirement $M_{j_1 j_2} > 100$ GeV to accept the jets associated with vector boson fusion: $q\bar{q} \rightarrow q'\bar{q}'h$. The results were not as promising as those based on cuts (a)–(c), and so we did not include a $M_{j_1 j_2} > 100$ GeV acceptance cut in our analysis.

In Table III we show the signal and differential cross-section rates after all cuts, including the $p_T^{\gamma\gamma} > M_{\gamma\gamma}/2$ and ‘‘vector boson acceptance’’ requirements. Table III can then be used to determine detectability of a Higgs boson given its mass and R_V :

$$R_V = \frac{\sigma(W/Z+h)B(h \rightarrow \gamma\gamma)}{\sigma(W/Z+h)_{\text{sm}}B(h \rightarrow \gamma\gamma)_{\text{sm}}}. \quad (13)$$

The parameter R_V is useful if we make the reasonable assumption that increases in $\sigma(W+h)$ and $\sigma(Z+h)$ scale equivalently.

In Fig. 4 we plot the 95% C.L. ($N_S=1.96$) exclusion curves for a given luminosity in the R_V-m_h plane. On the curve we have put lines for h_u^0 and the purely gauge coupled Higgs boson h_{bh}^0 . The SM Higgs boson corresponds to $R_V=1$ across the plot. For a given integrated luminosity, the region above the corresponding curve can be ruled out to 95% confidence level. The luminosity curves never cross $R_V=1$ which indicates that the SM Higgs boson could not be excluded in the $\gamma\gamma$ mode by the Tevatron even with 100 fb^{-1} of data. However, with 30 fb^{-1} one could exclude h_{bh}^0 up to 138 GeV and h_u^0 up to 131 GeV in the $\gamma\gamma$ channel alone. For $N_S=5$ discovery we plot in Fig. 5 the necessary enhancement of $B(h \rightarrow \gamma\gamma)$ to see a signal at this level at the Tevatron. Discovery is possible up to 128 GeV

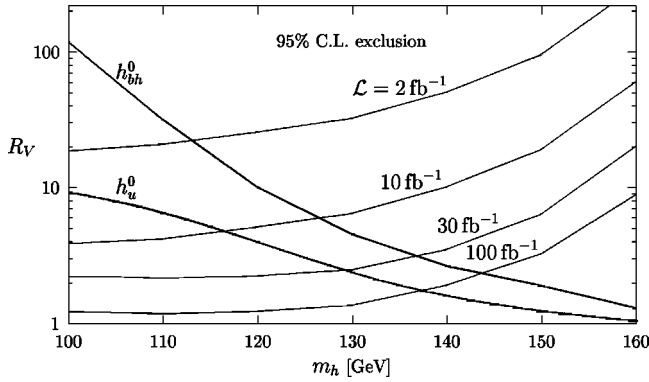


FIG. 4. 95% C.L. luminosity contours of Higgs boson detection in the R_V - m_h plane. For a given luminosity curve, the region below the curve cannot be ruled out with Tevatron data.

for the bosonic Higgs boson as long as at least 30 fb^{-1} is obtained, and h_u^0 can be discovered up to approximately 117 GeV. Both discovery reaches are beyond the expected reach capacity of LEP II.

DISCUSSION AND CONCLUSION

We have analyzed the capability of the Tevatron to find a Higgs boson decaying into two photons. We have found that the SM Higgs boson cannot be probed beyond LEP 2 capabilities if the Tevatron accrues less than 100 fb^{-1} . However, Higgs bosons in theories beyond the standard model may be probed (discovered or excluded) effectively with significantly less luminosity. For example, a Higgs boson that couples only to the vector bosons but has no couplings to the fermions can be probed up to 128 GeV with less than $\sim 10 \text{ fb}^{-1}$ integrated luminosity. In the minimal supersymmetric (MSSM), when $h \approx h_u^0$, so that $h \rightarrow b\bar{b}$ is suppressed and the $W/Z + h(\rightarrow b\bar{b})$ signal vanishes, our analysis shows coverage up to $m_h = 117 \text{ GeV}$ with 30 fb^{-1} and exclusion capability up to $m_h = 131 \text{ GeV}$.

In an attempt to be as model independent as possible, we have presented graphs (Figs. 2–5) of exclusion and detectability as integrated luminosity contours in the plane of Higgs boson mass and R_i (R_{gg} and R_V), where R_i param-

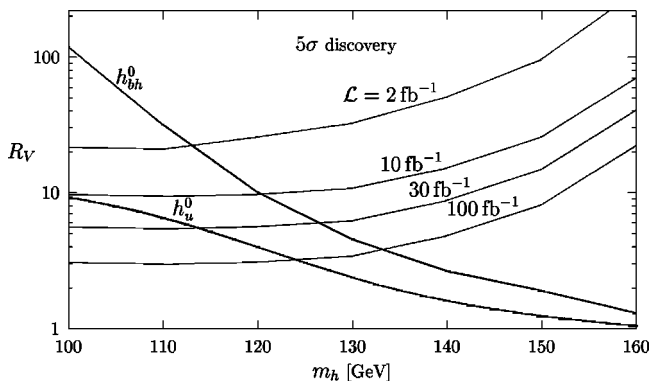


FIG. 5. 5σ discovery contours of Higgs boson detection in the R_V - m_h plane for a given luminosity. For each luminosity curve, the region above the curve can be discovered with Tevatron data.

eterizes the enhancement of the $\gamma\gamma$ signal cross section over the standard model. Therefore, any theories beyond the SM that have predictions for production cross sections and decay widths of Higgs bosons can be compared with these graphs to attain an estimate of the Tevatron's capability. Of course, these figures are not applicable to a Higgs boson that has an intrinsic width greater than the detector resolution. The theories discussed above are far from this case.

Finally, we comment on previous studies of $\gamma\gamma$ invariant mass signals at the Tevatron [21–26]. Much of the earlier work emphasized detectability at lower luminosities of h_{bh}^0 with $m_{h_{bh}^0} < 100 \text{ GeV}$, where the branching fraction to two photons was $\mathcal{O}(1)$. For example, this was the Higgs boson and the mass region covered in Ref. [21]. They also performed their simulations at the parton level and applied much looser cuts than our analysis and much looser than those typically used in the experimental analyses of $D\bar{D}$ and CDF in run I [16].

Another important analysis was completed very recently in Ref. [26] with results similar to ours, although the analysis differs in several ways (e.g., no $p_T^{\gamma\gamma}$ cut). This study suggests that a signal of two photons combined with a single jet or two jets is an effective method to search for a Higgs boson in the two photon decay mode, but it did not utilize cuts as stringent as ours. A careful comparison needs to be made among all the observables in the various studies under precisely the same assumptions to ascertain which observables are the most effective. And, of course, a combination of all useful observables should be employed to maximize our sensitivity to Higgs bosons. The suggested two photon observables outlined in this paper appear to be useful additions to the list of Higgs boson search observables.

ACKNOWLEDGEMENTS

J.W. thanks Lawrence Berkeley National Laboratory for partial support in the participating guest program. S.M. thanks G.L. Kane for useful conversations.

APPENDIX: ESTIMATION OF SIGNAL AND BACKGROUND

Signal

As mentioned in the text, we are mainly concerned with the processes $gg \rightarrow h$ and $q\bar{q} \rightarrow Vh$ (with $V=W$ or Z). The $gg \rightarrow h \rightarrow \gamma\gamma$ process is calculated based on b -space resummation (see, e.g., Ref. [27]), and performed to next-to-leading order (NLO) accuracy. The total event rates (without cuts) agree with other fixed order calculations [28]. Since the multiple, soft gluon emissions are integrated out, the effect of isolation cuts must be determined by some other means. We use a constant isolation efficiency per photon, $\epsilon_{\text{iso}} = 0.95$, for these inclusive studies. Our results can be easily scaled if necessary to account for a different efficiency.

The $q\bar{q} \rightarrow Vh$ process is calculated using PYTHIA [29], but multiplied by a constant K factor based on the resummed calculation of Ref. [30]. For completeness, the contribution of vector boson fusion processes was also calculated using

PYTHIA without any effective- W approximation and no K factor. This process was never relevant for our analysis, for reasons discussed in the main text.

Background

The background estimate of the inclusive production of $\gamma\gamma$ pairs—where kinematic cuts are applied only on the properties of the individual photons or the diphoton pair—uses the next-to-leading order, resummed calculation of Ref. [31] applied to the 2.0 TeV collider energy. Since the resummed calculation integrates out the history of the soft gluon emission, the photon isolation efficiency must be estimated by another means, such as a showering Monte Carlo simulation or from Z boson data. We use a constant isolation efficiency per photon $\epsilon_{iso}=0.95$ for the signal. No backgrounds from fragmentation photons (e.g. $\pi^0, \eta \rightarrow \gamma\gamma$) are included in our numbers. The results of Ref. [31] show good agreement with run I data, and contain only a small component of fragmentation photons. For simplicity, we have ignored it entirely. Of course, the actual contribution from fragmentation photons depends critically on the isolation criteria and on the minimum p_T^γ . Note that the resummed calculation *does* include the final state bremsstrahlung processes, e.g. $qg \rightarrow q\gamma\gamma$. We find that our calculational method

yields good agreement with the invariant mass distribution presented in Ref. [23] without a large fragmentation component.

To estimate the backgrounds to W or $Z+\gamma\gamma$, where the gauge bosons decay leptonically or hadronically, we need to determine the properties of the individual quarks and gluons emitted in the standard $\gamma\gamma$ production processes. This is not straightforward, since parton showering is accurate at describing event shapes but not event rates, whereas the hard NLO corrections to the $\gamma\gamma$ production rate are known to be important. For moderate values of $p_T^{\gamma\gamma}$ relative to $M_{\gamma\gamma}$, a fixed order (in α_s) calculation is as accurate in describing the kinematics of the photon pair as a resummed one (the transition between the two perturbative schemes is handled naturally in the resummation formalism, but the gluon emissions are integrated out). Therefore, we use the partonic subprocesses $q\bar{q} \rightarrow \gamma\gamma g$, $qg \rightarrow \gamma\gamma q$, etc., to set the event rate, plus the parton showering method to reconstruct the full history of possibly multiple gluon emissions. For the $gg \rightarrow \gamma\gamma$ jets background, we use parton showering with the $gg \rightarrow \gamma\gamma$ process, but using the improvements of Ref. [32] to approximate the NLO corrections (the effect of using the exact pentagon diagram for the $gg \rightarrow \gamma\gamma g$ process is not important [33]). The hard scale is set to the photon pair invariant mass. In all cases, we calculate the isolation efficiency explicitly.

-
- [1] For latest results, see <http://fnth37.fnal.gov/higgs.html>
- [2] A. Djouadi, J. Kalinowski, and M. Spira, *Comput. Phys. Commun.* **108**, 56 (1998).
- [3] M. Carena, J. R. Espinosa, M. Quiros, and C. E. Wagner, *Phys. Lett. B* **355**, 209 (1995); M. Carena, M. Quiros, and C. E. Wagner, *Nucl. Phys.* **B461**, 407 (1996); H. E. Haber, R. Hempfling, and A. H. Hoang, *Z. Phys. C* **75**, 539 (1997).
- [4] H. Baer and J. D. Wells, *Phys. Rev. D* **57**, 4446 (1998).
- [5] W. Loinaz and J. D. Wells, *Phys. Lett. B* **445**, 178 (1998).
- [6] M. Carena, S. Mrenna, and C. E. Wagner, *Phys. Rev. D* **60**, 075010 (1999).
- [7] M. Carena, S. Mrenna, and C. E. Wagner, *Phys. Rev. D* **62**, 055008 (2000).
- [8] L. J. Hall, R. Rattazzi, and U. Sarid, *Phys. Rev. D* **50**, 7048 (1994).
- [9] M. Dine, Y. Nir, and Y. Shirman, *Phys. Rev. D* **55**, 1501 (1997).
- [10] H. E. Haber, G. L. Kane, and T. Sterling, *Nucl. Phys.* **B161**, 493 (1979); J. F. Gunion, R. Vega, and J. Wudka, *Phys. Rev. D* **42**, 1673 (1990); B. Grzadkowski and J. F. Gunion, *Phys. Lett. B* **473**, 50 (2000).
- [11] J. D. Wells, *Phys. Rev. D* **56**, 1504 (1997).
- [12] C. T. Hill, *Phys. Lett. B* **266**, 419 (1991); *ibid.* **345**, 483 (1995).
- [13] M. Spira, A. Djouadi, D. Graudenz, and P. M. Zerwas, *Nucl. Phys.* **B453**, 17 (1995).
- [14] G. L. Kane, G. D. Kribs, S. P. Martin, and J. D. Wells, *Phys. Rev. D* **53**, 213 (1996).
- [15] A. Djouadi, *Phys. Lett. B* **435**, 101 (1998).
- [16] DØ Collaboration, S. Abachi *et al.*, *Phys. Rev. Lett.* **78**, 2070 (1997); CDF Collaboration, F. Abe *et al.*, *ibid.* **81**, 1791 (1998); CDF Collaboration, F. Abe *et al.*, *Phys. Rev. D* **59**, 092002 (1999); DØ Collaboration, B. Abbott *et al.*, *Phys. Rev. Lett.* **82**, 2244 (1999).
- [17] M. Spira and J. D. Wells, *Nucl. Phys.* **B523**, 3 (1998).
- [18] L. Hall and C. Kolda, *Phys. Lett. B* **459**, 213 (1999).
- [19] OPAL Collaboration, G. Abbiendi *et al.*, *Phys. Lett. B* **464**, 311 (1999).
- [20] S. Abdullin, M. Dubinin, V. Ilyin, D. Kovalenko, V. Savrin, and N. Stepanov, *Phys. Lett. B* **431**, 410 (1998).
- [21] A. Stange, W. Marciano and S. Willenbrock, *Phys. Rev. D* **49**, 1354 (1994).
- [22] A. G. Akeroyd, *Phys. Lett. B* **368**, 89 (1996).
- [23] CDF Collaboration, P. J. Wilson *et al.*, presented at the 29th International Conference on High-Energy Physics (ICHEP 98), Vancouver, British Columbia, Canada, 1998, Report No. Fermilab-Conf-98/213-E.
- [24] M. C. Gonzalez-Garcia, S. M. Lietti, and S. F. Novaes, *Phys. Rev. D* **57**, 7045 (1998).
- [25] R. Casalbuoni, A. Deandrea, S. De Curtis, D. Dominici, R. Gatto, and J. F. Gunion, *Nucl. Phys.* **B555**, 3 (1999).
- [26] G. Landsberg and K. T. Matchev, *Phys. Rev. D* **62**, 035004 (2000).
- [27] C. Balazs and C. P. Yuan, *Phys. Lett. B* **478**, 192 (2000).
- [28] M. Spira, “HIGLU: A Program for the Calculation of the Total Higgs Production Cross Section at Hadron Colliders via Gluon Fusion including QCD Corrections,” hep-ph/9510347.
- [29] T. Sjostrand, *Comput. Phys. Commun.* **82**, 74 (1994).
- [30] S. Mrenna and C. P. Yuan, *Phys. Lett. B* **416**, 200 (1998).
- [31] C. Balazs, E. L. Berger, S. Mrenna, and C. P. Yuan, *Phys. Rev. D* **57**, 6934 (1998).
- [32] S. Mrenna, “Higher order corrections to parton showering from resummation calculations,” hep-ph/9902471.
- [33] C. Balazs (private communication).